JACS
JOURNAL OF THE AMERICAN CHEMICAL SOCIETY

ARTICLE

pubs.acs.org/JACS

ENDOR/HYSCORE Studies of the Common Intermediate Trapped during Nitrogenase Reduction of N_2H_2, CH_3N_2H, and N_2H_4 Support an Alternating Reaction Pathway for N_2 Reduction

Dmitriy Lukoyanov,[‡] Sergei A. Dikanov,[*,⊥] Zhi-Yong Yang,[∥] Brett M. Barney,[∥,△] Rimma I. Samoilova,[†] Kuppala V. Narasimhulu,[⊥] Dennis R. Dean,[*,§] Lance C. Seefeldt,[*,∥] and Brian M. Hoffman[*,‡]

[‡]Department of Chemistry, Northwestern University, Evanston, Illinois 60208, United States

[⊥]Department of Veterinary Clinical Medicine, University of Illinois, Urbana, Illinois 61801, United States

[∥]Department of Chemistry and Biochemistry, Utah State University, Logan, Utah 84322, United States

[†]Institute of Chemical Kinetics and Combustion, Russian Academy of Sciences, Novosibirsk 630090, Russian Federation

[§]Department of Biochemistry, Virginia Tech, Blacksburg, Virginia 24061, United States

Supporting Information

ABSTRACT: Enzymatic N_2 reduction proceeds along a reaction pathway composed of a sequence of intermediate states generated as a dinitrogen bound to the active-site iron−molybdenum cofactor (FeMo-co) of the nitrogenase MoFe protein undergoes six steps of hydrogenation (e^-/H^+ delivery). There are two competing proposals for the reaction pathway, and they invoke different intermediates. In the 'Distal' (D) pathway, a single N of N_2 is hydrogenated in three steps until the first NH_3 is liberated, and then the remaining nitrido-N is hydrogenated three more times to yield the second NH_3. In the 'Alternating' (A) pathway, the two N's instead are hydrogenated alternately, with a hydrazine-bound intermediate formed after four steps of hydrogenation and the first NH_3 liberated only during the fifth step. A recent combination of X/Q-band EPR and ^{15}N, $^{1,2}H$ ENDOR measurements suggested that states trapped during turnover of the α-70^{Ala}/α-195^{Gln} MoFe protein with diazene or hydrazine as substrate correspond to a common intermediate (here denoted **I**) in which FeMo-co binds a substrate-derived $[N_xH_y]$ moiety, and measurements reported here show that turnover with methyldiazene generates the same intermediate. In the present report we describe X/Q-band EPR and $^{14/15}N$, $^{1,2}H$ ENDOR/HYSCORE/ESEEM measurements that characterize the N-atom(s) and proton(s) associated with this moiety. The experiments establish that turnover with N_2H_2, CH_3N_2H, and N_2H_4 in fact generates a common intermediate, **I**, and show that the N−N bond of substrate has been cleaved in **I**. Analysis of this finding leads us to conclude that nitrogenase reduces N_2H_2, CH_3N_2H, and N_2H_4 via a common A reaction pathway, and that the same is true for N_2 itself, with Fe ion(s) providing the site of reaction.

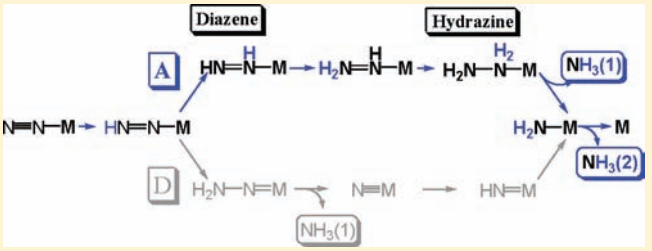

Nitrogen fixation, the reduction of N_2 to two NH_3 molecules, is essential for all life, with the lives of over one-half of today's human population depending on biologically fixed nitrogen.[1] Biological nitrogen fixation, which requires energy in the form of MgATP, is catalyzed by the enzyme nitrogenase according to the limiting stoichiometry:[2,3]

$$N_2 + 8e^- + 8H^+ + 16MgATP \rightarrow 2NH_3 + H_2 + 16MgADP + 16Pi \quad (1)$$

There are three types of nitrogenases,[4] with the best-characterized and most prevalent being the Mo-dependent enzyme studied here.[3,5,6] It consists of two components, denoted the Fe protein and the MoFe protein. The former delivers electrons to the catalytic MoFe protein, which contains two remarkable metal clusters, the N_2 binding/reduction active site, the iron−molybdenum cofactor ([7Fe-9S−Mo-X-homocitrate]; FeMo-co, Figure 1), and the [8Fe-7S] P cluster, which is involved in electron transfer to FeMo-co.[3,5]

N_2 reduction by nitrogenase proceeds along a reaction pathway composed of the sequence of intermediate states generated as a dinitrogen bound to FeMo-co undergoes six steps of hydrogenation (e^-/H^+ delivery),[2,3,5−8] as depicted in the Lowe−Thorneley kinetic model for nitrogenase function.[3,9,10] We note that one can further consider whether electron/proton delivery at each stage is coupled or sequential, thereby possibly introducing additional intervening intermediates,[11] but such issues are beyond the scope of this report.

Two competing proposals for the reaction pathway have long been considered.[3,6,12] They invoke distinctly different intermediates, Scheme 1, and computations suggest they likely involve

Received: April 19, 2011
Published: July 11, 2011

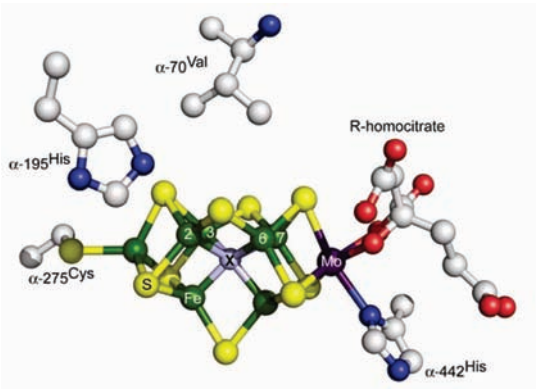

Figure 1. Structure of FeMo-co showing Fe green, Mo purple, S yellow, X gray.

Scheme 1

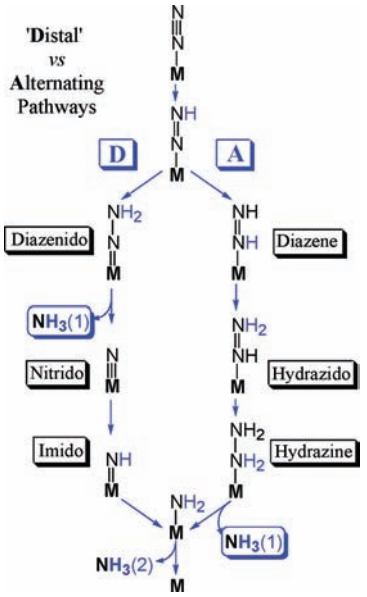

different metal-ion sites on FeMo-co.[12] In the 'Distal' (D) pathway, followed by N_2-fixing inorganic Mo complexes[11] and suggested to apply in reaction at Mo of FeMo-co,[13] a single N of N_2 is hydrogenated in three steps until the first NH_3 is liberated, and then the remaining nitrido-N is hydrogenated three more times to yield the second NH_3. In the 'Alternating' (A) pathway that has been suggested to apply to reaction at Fe of FeMo-co,[14] the two N's instead are hydrogenated alternately, with a hydrazine-bound state generated upon four steps of hydrogenation and the first NH_3 only liberated during the fifth step. Simple arguments can be made for both pathways. For example, the A route is suggested by the fact that hydrazine is both a substrate of WT nitrogenase and is released upon acid or base hydrolysis of the enzyme under turnover,[3,8,15] and is favored in computations with reaction at Fe,[12,14] while the D route is suggested by the fact that the only inorganic complexes that catalytically fix N_2 employ Mo and function via the D route,[11] which is computationally favored for reaction at Mo.[12] As shown by Scheme 1, characterization of catalytic intermediates can distinguish between the two competing pathways.

Nitrogenase reduction intermediates had long eluded capture until we[5,16,17] described the freeze-trapping and ENDOR spectroscopic studies of a number of them, each of which shows an EPR signal arising from an $S = 1/2$ state of the FeMo-co, rather than the $S = 3/2$ state of resting-state FeMo-co.[5] These include intermediates formed during the reduction of alkyne substrates,[18] the reduction of H^+ under Ar,[19] and finally, four associated with N_2 fixation itself.[16,17,20−24] These four include a proposed early (e) stage of the reduction of N_2, e(N_2), obtained from wild-type (WT) MoFe protein with N_2 as substrate,[16] and three putative 'midstage' or late-stage intermediates that are the subject of this study: m(NH═N−CH_3), obtained from α-195^{Gln} MoFe protein with CH_3−N═NH as substrate;[23] m(NH═NH), obtained from the doubly substituted, α-70^{Ala}/α-195^{Gln} MoFe protein during turnover with in situ-generated NH═NH,[17] and a 'late' stage, l(N_2H_4), from the α-70^{Ala}/α-195^{Gln} MoFe protein during turnover with H_2N-NH_2[21] as substrate.

Both hydrazine and diazene are substrates of wild-type nitrogenase that, like N_2, are reduced to ammonia.[3,17,21] Substitution of the α-70^{Val} residue by α-70^{Ala} opens up the active site in the vicinity of an Fe ion at the waist of FeMo-co, Fe6, to accommodate larger substrates, increasing the rate of ammonia formation when either hydrazine or diazene is the substrate[5] and implicating Fe as the site of substrate binding. Substitution of the α-195^{His} residue by α-195^{Gln}, alone or in combination with the α-70^{Ala} substitution, is thought to disrupt the delivery of protons for reduction of nitrogenous substrates[25] and facilitate the accumulation of intermediates.[5] Recently, a combination of X/Q-band EPR and ^{15}N, $^{1,2}H$ ENDOR measurements suggested that m(NH═NH) and l(N_2H_4) formed during turnover of the α-70^{Ala}/α-195^{Gln} MoFe protein with diazene or hydrazine as substrate correspond to a common intermediate (here denoted **I**) in which FeMo-co binds a substrate-derived [N_xH_y] moiety.[17] However, whether or not the N−N bond in **I** had been broken (x = 1 or 2) was not established. The capture of a common intermediate would indicate that diazene and hydrazine both enter and 'flow through' the normal N_2-reduction pathway (Scheme 1), and that the diazene-derived intermediate is not 'midstage', but rather that diazene must have 'caught up' with the 'later' hydrazine reaction via additional steps of enzymatic hydrogenation.

In the present report we describe X/Q-band EPR and $^{14/15}N$, $^{1,2}H$ ENDOR/HYSCORE/ESEEM[26−28] measurements that characterize the N-atom(s) and proton(s) associated with the substrate-derived moiety of the intermediates formed during turnover with N_2H_2 and N_2H_4, and further report measurements of the intermediate trapped during turnover with NH═N−CH_3, which can be selectively ^{15}N labeled in either nitrogen. These measurements establish that all three substrates generate a common intermediate, **I**, in which the N−N bond of substrate has been cleaved. Consideration of this finding allows us to evaluate whether the D or A reduction pathways (Scheme 1) describes N_2 fixation by nitrogenase, and which type of metal ion, Fe or Mo, forms the reactive site.

MATERIALS AND METHODS

Samples. The preparation of the MoFe α-70^{Ala}/α-195^{Gln} protein and the freeze-trapping of intermediates for paramagnetic resonance measurements have been described.[17,21,23]

Q-Band CW and Pulsed ENDOR Experiments. CW and pulsed 35 GHz ENDOR spectra were recorded at 2 K as described

previously.[17,21,23] The ENDOR spectrum for a single orientation of an $I = 1/2$ nucleus (^{1}H, ^{15}N) is a $\nu_\pm$ doublet centered at the nuclear Larmor frequency and split by the hyperfine coupling, A; hyperfine tensors are obtained through analysis of 2D field-frequency plots composed of spectra collected at multiple fields across the EPR envelope.[27,29] Pulsed ENDOR spectra were detected with Mims and ReMims sequences.[30] Intensity of ENDOR response for Mims sequence, [π/2-τ-π/2-T(rf)-π/2-τ-detect], follows the relationship, $I(A) \sim 1 - \cos(2\pi A\tau)$, and as a result, the signals at $A\tau = n$, $n = 0, 1, \ldots$ are suppressed ('blind spots'). ReMims sequence, [π/2-τ_1-π/2-T(rf)-π/2-τ_2-π-(τ_1+τ_2)-detect], allows using short preparation interval τ_1 and study of a wider range of hyperfine values without 'blind spot' distortions.

X-Band Pulsed EPR and ESEEM Experiments. CW EPR measurements were performed on an ESP 300 Bruker spectrometer equipped with Oxford CF 935 cryostat. Pulsed X-band EPR measurements were carried out using a Bruker ELEXSYS E580 spectrometer with an Oxford CF 935 cryostat at 8 K. Several types of ESEEM experiments with different pulse sequences were employed, with appropriate phase-cycling schemes to eliminate unwanted features from experimental echo envelopes. Among them are two-pulse and one-(1D) and two-dimensional (2D) four-pulse sequences. In the two-pulse experiment (π/2-τ-π-τ-echo), the intensity of the echo signal is measured as a function of the time interval τ between two microwave pulses with turning angles $\pi/2$ and π to generate an echo envelope that maps the time course of relaxation of the spin system (in ESEEM) or as a function of magnetic field at fixed τ (in field-sweep ESE). In the 2D four-pulse HYSCORE experiment (π/2-τ-π/2-t_1-π-t_2-π/2-τ-echo),[31] the intensity of the echo after the fourth pulse was measured with t_2 and t_1 varied and τ constant. The length of a $\pi/2$ pulse was nominally 16 ns and a π pulse 32 ns. The repetition rate of pulse sequences was 1000 Hz. HYSCORE data were collected in the form of 2D time-domain patterns containing 256 × 256 points with steps of 20 or 32 ns. Spectral processing of ESEEM patterns, including subtraction of the relaxation decay (fitting by polynomials of 3−6 degrees), apodization (Hamming window), zero filling, and fast Fourier transformation (FT), was performed using Bruker WIN-EPR software.

RESULTS

In describing results, we will employ the original notation, m(NH═NH), m(NH═N−CH_3), and l(N_2H_4), when it is helpful in specifying the origin of a sample and/or its isotopic composition for ENDOR/HYSCORE measurements. As these in fact represent a common intermediate, when discussing properties we will commonly refer to it as **I**.

X- and Q-Band EPR. EPR spectra of α-70^{Ala}/α-195^{Gln} trapped during turnover in the presence of N_2H_4 and N_2H_2 reveal a complete disappearance of the resting state spectrum and the presence of the low-spin signal with almost axial **g**-tensor characteristic of the **I** intermediate. For completeness, we note that the high field part of the **I** spectrum is overlapped with the rhombic signal of the reduced 4Fe4S cluster of the Fe protein, $g = [2.05, 1.94, 1.86]$. As shown earlier, the spectrum of **I** is the sum of contributions from two conformers.[17] X-band and Q-band spectra of the m(NH═N−CH_3) intermediate formed by turnover of CH_3N_2H with α-70^{Ala}/α-195^{Gln} MoFe protein likewise show the presence of two major conformers and their g-values are indistinguishable from those of the l(N_2H_4), suggesting that enzymatic turnover with methyldiazene likewise generates intermediate **I**.

We have also extended the characterization of the spin properties of **I**. The temperature and microwave power dependencies of the l(N_2H_4) signal show that the two major conformers of the EPR-active FeMo-co in **I** have significantly different relaxation properties, Figure 2. At temperatures below 8 K, the X-band signal is dominated by a conformer with **g** = [2.09, 2.01, 1.98] (g_1 = 2.09 signal), Figure 2. As the temperature is increased to $T \sim 15$ K, the EPR signal from a second conformer with $g_1 = 2.11$ becomes dominant. The signal intensity decreases at still higher temperatures, disappearing above $T \sim 30$ K.

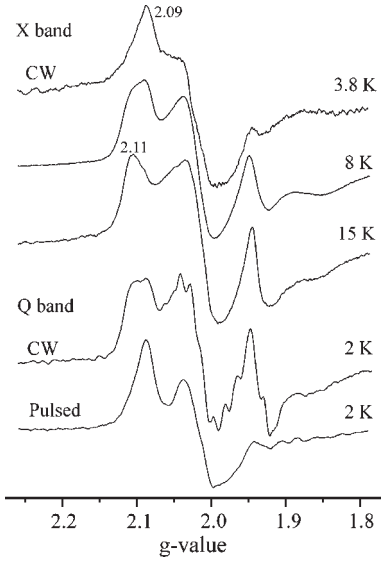

Figure 2. EPR spectra of intermediate **I** (l(N_2H_4)) detected by various techniques. Conditions for CW X-band: microwave frequency, 9.38 GHz; microwave power, 10 mW; modulation amplitude, 7 G; time constant, 160 ms; field sweep speed, 20 G/s. Conditions for CW Q-band: microwave frequency, 35.08 GHz; microwave power, 32 μW; modulation amplitude 4 G; time constant, 128 ms; field sweep speed, 17 G/s. Conditions for pulsed Q-band: microwave frequency, 34.79 GHz; Mims sequence, $\pi/2 = 50$ ns, $\tau = 600$ ns; repetition time 10 ms, 50 shots/point; field sweep speed, 8 G/s.

Q-band CW spectra collected at $T = 2$ K show signals from both major conformers at high microwave power. As the power is lowered, the $g_1 = 2.11$ signal progressively becomes more prominent. At the microwave power settings used for 2 K Q-band CW ^{1}H ENDOR measurements, the conformers contribute roughly equally to the EPR spectrum, Figure 2. In contrast, the 2 K Q-band echo-detected EPR spectrum collected with the short repetition times (∼10 ms) used for ^{15}N Mims pulsed ENDOR experiments is dominated by the $g_1 = 2.09$ conformer, which thus governs these ENDOR measurements. The contribution of the $g_1 = 2.11$ conformer becomes more noticeable with longer repetition times (∼50 ms) but remains substantially lower in intensity.

On the basis of the temperature dependence of the CW X-band EPR spectra, Figure 2, it is likely that the two conformers contribute roughly equally at the temperatures used to collect X-band HYSCORE spectra, $T \approx 8$ K. For completeness, Figure S1 shows the X-band field-sweep two-pulse ESE spectrum. It is a broad line between 322.0 mT and 382.0 mT with two maxima around 345.0 mT and 360.0 mT corresponding to $g = 2.01$ and 1.926, respectively. The relative intensities of two maxima varied slightly in different samples used in this work, presumably because of slight variations in the ratio of Fe to MoFe proteins.

35 GHz ^{1}H CW and ^{2}H Pulsed ENDOR. The 35 GHz CW ^{1}H ENDOR spectra at $g = 2.02$ for l(N_2H_4) in H_2O buffer show a peak corresponding to the higher-frequency, ν_+, branch of the

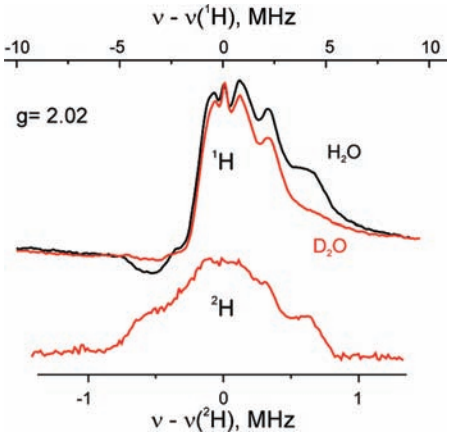

Figure 3. 35 GHz CW ^{1}H ENDOR spectra of **I** (l(N_2H_4)) obtained at g = 2.02 for samples prepared in H_2O (black) and D_2O (red) buffers. The lower spectrum shows pulsed ^{2}H ENDOR detected for D_2O sample. Conditions for CW ENDOR: microwave frequency, 35.002 GHz (H_2O), 35.096 GHz (D_2O); modulation amplitude, 2.5 G; time constant, 64 ms; bandwidth of RF broadened to 100 kHz; RF sweep speed, 1 MHz/s, 80 scans; temperature, 2 K. Conditions for pulsed ENDOR: microwave frequency, 34.886 GHz; Mims sequence, $\pi/2$ = 52 ns, τ= 452 ns; RF 73 μs; repetition time 12 ms, 16 shots/point, 32 scans; temperature, 2 K.

doublet for a proton(s) with $A(1) \sim 8$ MHz, a shoulder from a proton(s) with $A(2) \sim 6$ MHz, and a central, poorly resolved signal with breadth of ~4 MHz. The ν_- branch of the H1 and H(2) spectra are, respectively, distorted and absent, common observations in such low-temperature spectra. When l(N_2H_4) is prepared in D_2O buffer, the H1 signal is lost and instead is visible in the ^{2}H Mims pulsed ENDOR spectrum, Figure 3. Although the ^{2}H spectrum has a hint of a $\nu_+(2)$ feature, suggesting H(2) likewise is exchangeable, the H(2) shoulder is not lost from the sample prepared in D_2O buffer, so we conclude that H(2) is not exchangeable. In addition, although the majority of the central peak is not lost with D_2O buffer, and hence not exchangeable, the ^{2}H spectrum shows that a fraction of it does exchange. The coupling, A(1) decreases as the field is increased/decreased toward g_3/g_1. At these single-crystal orientations, the signals are strongly overlapped with the broad peak of weakly coupled protons, and minimum hyperfine coupling can only be roughly estimated as $A(1)_{min} \lesssim 6$ MHz. The poor resolution of the H1 ENDOR signals likely arises from the presence of multiple slightly inequivalent H1 protons plus the presence of two distinct conformers. The maximum component of the hyperfine tensor, $A(1)_{max} \sim 9$ MHz, occurs at $g \sim 2.05$ (Figure S2). If the field dependence of the poorly resolved H1 ENDOR pattern is considered to be associated with an anisotropic interaction of the dipolar form, the polar angle between dipolar direction and g_1 is estimated to be $\theta \sim 45°$.

9 GHz ^{1,2}H ESEEM/HYSCORE. Weak hyperfine couplings of the protons around FeMo-co and 4Fe4S centers were studied using orientation-selective two-dimensional ESEEM, called HYSCORE. The HYSCORE experiment creates off-diagonal cross-peaks (ν_α, ν_β) and (ν_β, ν_α) from each I = 1/2 nucleus in the 2D spectrum. Powder and orientation-selected HYSCORE spectra of I = 1/2 nuclei reveal, in the form of cross-ridges, the interdependence between ν_α and ν_β, in the same orientations. Analysis of the ridges in $(\nu_\alpha)^2$ vs $(\nu_\beta)^2$ coordinates allows separate estimate of the isotropic (a) and anisotropic (T) components of the hyperfine tensors.[32]

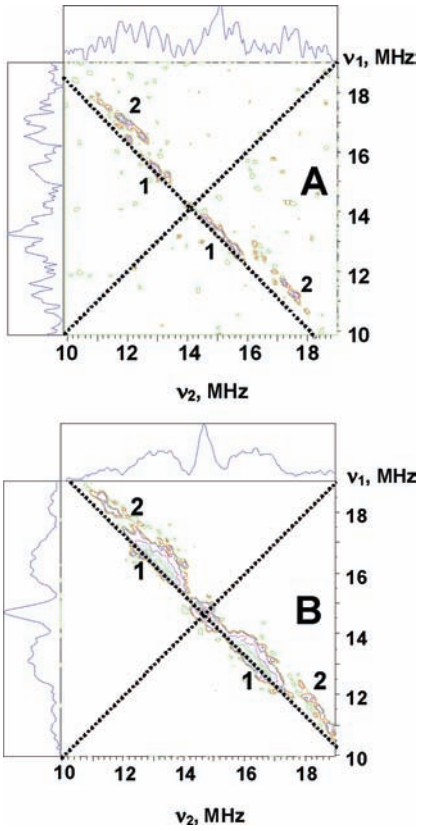

Figure 4. Contour presentations of the ^{1}H HYSCORE spectra of the l(N_2H_4) intermediate (magnetic field 332.0 mT (A) and 345.0 mT (B), time between first and second pulses τ = 136 ns, microwave frequency 9.6982 GHz).

Figure 4 shows ^{1}H HYSCORE spectra of the l(N_2H_4) intermediate obtained at the magnetic field 332.0 mT (g = 2.087) (Figure 4A) and 334.5 mT (g = 2.008) (B). Spectra resolve two pairs of cross-peaks **1** and **2**. Cross-peaks **2** possess larger splitting ~6−8 MHz and visible deviation from antidiagonal, indicating a significant anisotropic hyperfine component. The intensities of the cross-peaks **2** decrease relative to those of **1**, as the magnetic field is increased and cross-peaks **2** are not observed above ~349.0 mT (g = 1.985). Cross-peaks **2** were also not observed in the spectra of the sample prepared in D_2O, showing that they are produced by exchangeable proton(s). As discussed in detail in Supporting Information, quantitative analysis of the cross-ridge **2** contours from the spectra recorded at different field in the coordinates $(\nu_1)^2$ vs $(\nu_2)^2$ using methodology previously described[33] and assuming an axial anisotropic component gives two possible solutions: T = 4.6 MHz, a = −0.2 MHz and T = 4.6 MHz, a = −4.3 MHz (signs are relative). These values for a and T correspond to $A_\perp = |a - T| \sim 4.8$ MHz and $A_{||} = |a + 2T| \sim 9$ MHz for the first solution, and $A_\perp \sim 9$ MHz and $A_{||} \sim 4.8$ MHz for the second. The second solution is consistent with the observation in Q-band ENDOR of an exchangeable proton(s) with maximum coupling, $A(1)_{max} \sim 9$ MHz and minimum coupling, $A(1)_{min} \lesssim 6$ MHz. Cross-peaks **1** correspond to the nonexchangeable proton shoulder seen in Q-band ENDOR and associated with the protein.

Additional information about the exchangeable proton(s) was sought from 1D four-pulse ^{1}H ESEEM spectra. Such spectra contain lines in the region of the double proton Larmor frequency

($2\nu_H \sim 28-29$ MHz) that are sum-combination harmonics ($\nu_\alpha + \nu_\beta$) of two basic frequencies ν_α and ν_β. As presented in Supporting Information, analysis of these harmonics shows the existence of protons with the same anisotropic coupling as found for the exchangeable protons by HYSCORE.

35 GHz ^{15}N ReMims ENDOR. Figure 5A presents pulsed ^{15}N ENDOR spectra collected at selected *g*-values for the intermediates trapped during turnover with the three isotopically labeled substrates, N_2H_2, CH_3N_2H, and N_2H_4, and Figure 5B presents a 2D field-frequency plot of pulsed ^{15}N ENDOR spectra collected across the EPR envelope of l($^{15}N_2H_4$) prepared from the α-70^{Ala}/α-195^{Gln} MoFe protein by freeze-quench during turnover in the presence of $^{15}N_2H_4$. Spectra were collected with the ReMims[30] pulse sequence. This permitted measurements with τ_1 = 200 ns, which eliminates Mims ENDOR 'blind spots' from the frequency range of the scan. Wider ENDOR scans collected for l($^{15}N_2H_4$) showed no ^{15}N signal with a hyperfine coupling greater than the maximum for N1, A_3 = 2.7 MHz.

The spectra for the three intermediates are essentially identical, Figure 5A. The observed 2D ^{15}N ENDOR patterns, as shown for l($^{15}N_2H_4$), Figure 5B, is consistent with the presence of a single type of ^{15}N. As shown in Figure 5, the 2D pattern can be described moderately well by simulations that assume a single ^{15}N with hyperfine tensor, **A**(^{15}N1) = ±[1, 1.5, 2.8] MHz, $|a_{iso}(^{15}N1)|$ = 1.8 MHz, corresponding to **A**(^{14}N1) = ±[0.7, 1.1, 2] MHz, $|a_{iso}(^{14}N1)|$ = 1.3 MHz. The observation of an isotropically coupled, substrate-derived ^{15}N signal, in conjunction with the observation of the exchangeable H1 ENDOR signal, establishes the presence of a substrate-derived [N_xH_y] moiety bound to metal ion(s) of the cofactor of **I**. These pulsed-ENDOR measurements were performed at *T* = 2 K with a 10 ms repetition time. As shown in Figure 2, the EPR spectrum collected under these conditions is dominated by the g_1 = 2.09 conformer. Thus, the ^{15}N1 hyperfine tensor derived from the ReMims pulsed ENDOR measurements are assigned to this conformer, whose **g** tensor was used in the simulation.

The imperfections to the simulations in Figure 5B in terms of a single ^{15}N1 associated with each FeMo-co can be attributed to a combination of two factors: a distribution in the N1 tensor values for the g_1 = 2.09 dominant conformer; a contribution from the ^{15}N1 associated with the g_1 = 2.11 conformer, whose contribution to the EPR spectrum can be discerned in Figure 2. The ^{15}N ENDOR spectra of m(^{15}NH═N−CH_3), Figure 5A, confirm that the spectra do *not* instead arise from an overlap of signals from two nearly equivalent ^{15}N associated with each FeMo-co. The original study of this intermediate,[23] which employed the α-195^{Gln}-substituted MoFe protein and not the double mutant employed in this study, showed that when m(^{15}NH═N−CH_3) is formed from ^{15}NH═N−CH_3 it exhibits a ^{15}N signal comparable to those of N_2H_4 and N_2H_2, but with a slightly smaller coupling, $|a_{iso}(^{15}N1)| \approx$ 1.5 MHz. To ensure proper comparisons, we here examine m(^{15}NH═N−CH_3) generated with the α-70^{Ala}/α-195^{Gln} MoFe protein, as with the other two substrates.

The EPR signal of m(^{15}NH═N−CH_3) prepared with the α-70^{Ala}/α-195^{Gln} MoFe protein is reported above to be the same as that of **I**, and Figure 5A likewise demonstrates that the ReMims ENDOR spectra of m(^{15}NH═N−CH_3) are the same as those of **I** formed with $^{15}N_2H_4$ and $^{15}N_2H_2$. The EPR and ENDOR results together therefore establish that turnover with methyldiazene also generates the common intermediate, **I**. As there is only one ^{15}N in this substrate, the ^{15}N signal for **I** cannot come

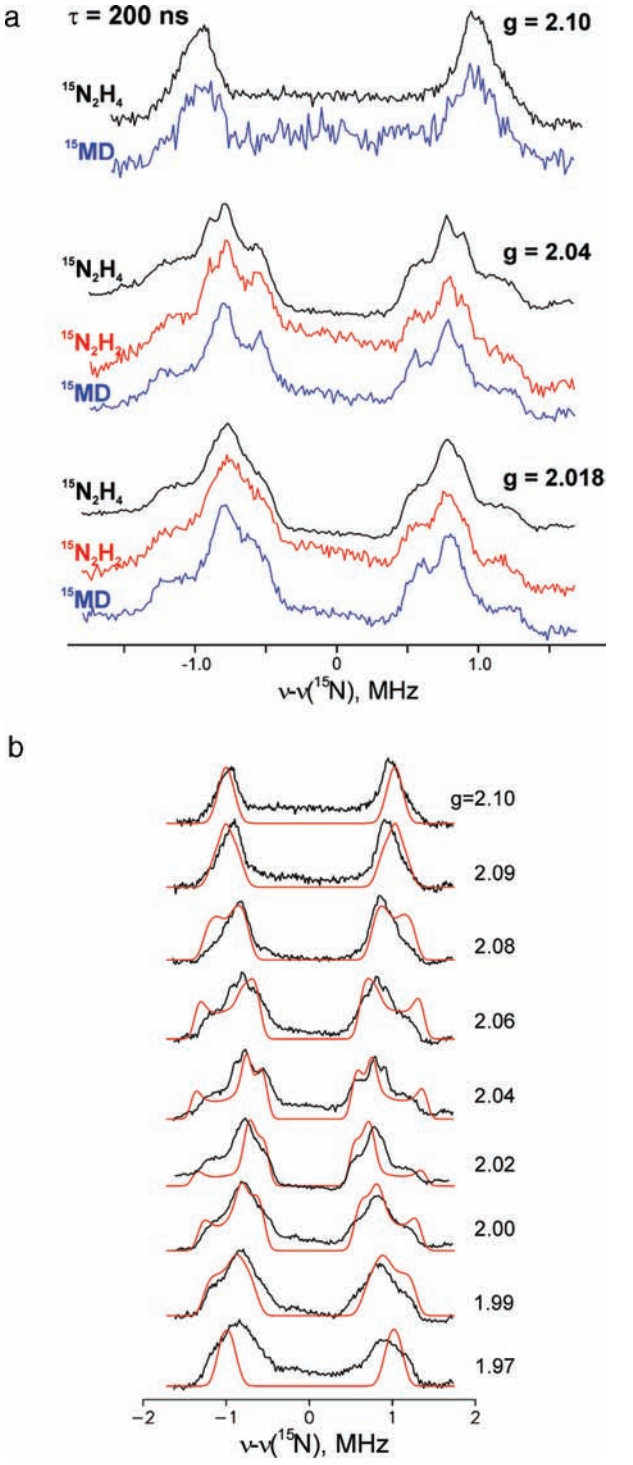

Figure 5. (A) Comparison of 35 GHz ReMims pulsed ^{15}N ENDOR spectra of intermediates trapped during turnover of the α-70^{Ala}/α-195^{Gln} MoFe protein with $^{15}N_2H_4$, $^{15}N_2H_4$, and ^{15}NH═N−CH_3 (denoted ^{15}MD). (B) 2D Field-frequency plot of 35 GHz pulsed ^{15}N ENDOR spectra of l($^{15}N_2H_4$) intermediate. Conditions: microwave frequency, 34.82 GHz; ReMims sequence, $\pi/2$ = 30 ns, τ_1 = 200 ns; RF 40 μs; repetition time, 10 ms; 500−950 scans; temperature, 2 K. Spectral baselines were corrected by simple subtraction if needed. Simulation (red) parameters: *g* = [2.09, 2.015, 1.98], hyperfine tensor **A** = [1.0, 2.8, 1.5] MHz, Euler angles φ = 50°, θ = 60°, ψ = 55° with respect to *g*-frame.

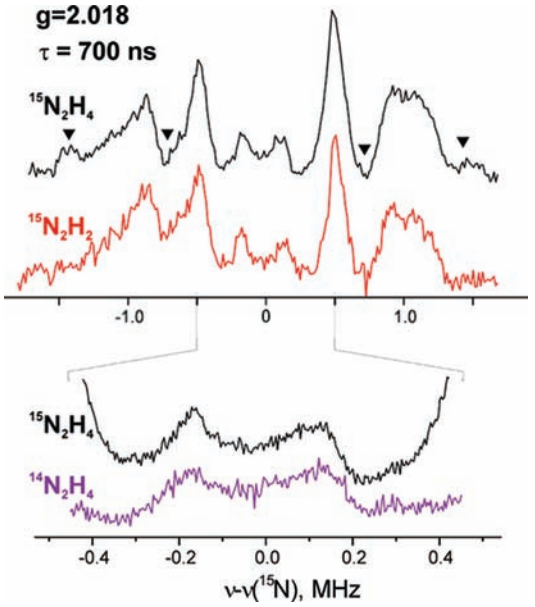

Figure 6. 35 GHz Mims ^{15}N ENDOR spectra detected at the maximum of EPR signal intensity (g_2 = 2.018) for l($^{15}N_2H_4$) (black) and m($^{15}N_2H_2$) (red) intermediates. Expanded spectra, below, compare the region around ^{15}N Larmor frequency for l($^{15}N_2H_4$) (black) and l($^{14}N_2H_4$) (purple) Spectra are shown after simple baseline correction; triangles represent distortions induced by "blind spots" of Mims ENDOR. Conditions: microwave frequency, ~34.82 GHz; Mims sequence, $\pi/2$ = 50 ns, τ = 700 ns; RF 40 μs; repetition time, 10 ms; 800−3800 scans; temperature, 2 K.

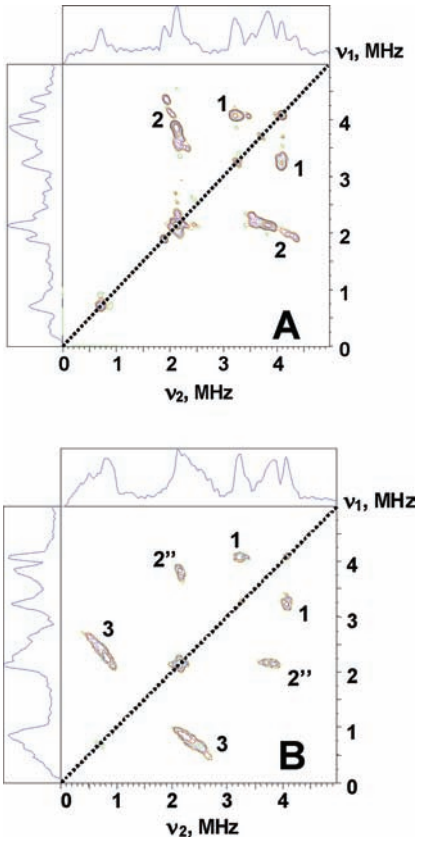

Figure 7. Contour presentations of the ^{14,15}N HYSCORE spectra of the l(N_2H_4) intermediate with $^{14}N_2H_4$ (A) and $^{15}N_2H_4$ (B) (magnetic field 345.9 mT ($^{14}N_2H_4$) and 346.0 mT ($^{15}N_2H_4$), time between first and second pulses τ=136 ns, microwave frequency 9.702 GHz ($^{14}N_2H_4$) and 9.707 GHz ($^{15}N_2H_4$).

from two nearly equivalent ^{15}N associated with each FeMo-co and must come from contributions from two conformers, each with a single ^{15}N bound to FeMo-co.

We may further conclude that the slight differences in hyperfine parameters for m(^{15}NH═N−CH$_3$) prepared with the α-195^{Gln} and the α-70^{Ala}/α-195^{Gln} MoFe proteins result from secondary influences, that turnover of NH═N−CH$_3$ indeed forms the common intermediate, **I**. With this identification, the previous study of **I** then further confirms that the signals of Figure 5A arise from a single ^{15}N bound to FeMo-co in each of two conformers: when **I** is formed from NH═^{15}N−CH$_3$ there is no such ^{15}N signal. The use of NH═N−CH$_3$ isotopomers thus proves that either the N−N bond has been cleaved in **I**, or an N_2H_x moiety from substrate binds end-on.

^{15}N Mims ENDOR. To test for end-on binding of N_2H_x, we examined the intermediates l($^{15}N_2H_4$) and, m($^{15}N_2H_2$) for the presence of a second ^{15}N derived from substrate, but with a smaller coupling than for N1, by collecting Mims ENDOR scans with a large pulse interval, τ. Although the signal from the latter sample is weaker, it is indistinguishable from that of the former, in keeping with the assignment of both to **I**. The intensity of the Mims ENDOR response for a signal with hyperfine coupling, A (MHz), depends on $\tau(\mu s)$ through the function, $I(\tau) \sim 1 - \cos(2\pi A\tau)$. When $A\tau = n$, the intensity is null and 'blind spots' appear in the ENDOR spectrum, as seen in the Mims spectrum taken for ^{15}N1 with τ = 700 ns, Figure 6. However, in parallel, $I(\tau)$ shows sensitivity maxima at $A\tau = n + 1/2$ and overall gives the best sensitivity at $A\tau \approx 1/2$. Thus, as τ is progressively increased, the measurements become progressively more sensitive to smaller values of A. As this is a relative sensitivity, measurements were performed at the maximum of EPR signal intensity (g_2).

Setting τ = 700 ns in the Mims sequence, Figure 6, not only introduces the holes in the ^{15}N1 spectra of l($^{15}N_2H_4$) and m($^{15}N_2H_2$) but also causes what *appears* to be a ^{15}N doublet from a second, weakly coupled ^{15}N from substrate, centered at ν_N, with A(^{15}N2) ~ 0.3 MHz. However, this signal remains unchanged when a corresponding spectrum is collected for l($^{14}N_2H_4$) (and m($^{14}N_2H_2$), not shown) prepared from $^{14}N_2H_4$ substrate. Thus, this ENDOR response is *not* associated with a second, weakly coupled ^{15}N2 of substrate and instead can be assigned as a double-quantum transition from ^{14}N associated with the MoFe protein. The narrow τ = 700 ns scan, collected with extremely high signal/noise, shows *no* trace of any ^{15}N ENDOR response from a weakly coupled ^{15}N. Considering the example of nitrile hydratase (NHY)[34] where a weakly coupled ^{15}N (A < 0.05 MHz) is reliably detectable, one can conclude that hyperfine couplings ratio for metal-bound ^{15}N1 and a possible second ^{15}N2 of substrate must be A(N1)/A(N2) > 40. As with the direct inferences drawn from the different isotopologues of methyldiazene, the absence of any trace of a weakly coupled ^{15}N2 indicates that the N−N bond of substrate N_2H_4 has been cleaved, and the ^{15}N1 and ^{1}H1 ENDOR signals are associated with an [N_1H_y] species.

^{14,15}N HYSCORE. HYSCORE experiments were performed with two samples of intermediate prepared from the α-70^{Ala}/α-195^{Gln}-substituted MoFe protein by use of $^{14}N_2H_4$ or $^{15}N_2H_4$ as substrate. Figure 7 shows representative HYSCORE spectra of two samples in the low frequency part appropriate for the weakly

coupled nitrogens. These spectra are recorded at the magnetic field corresponding to the low-field maximum $g = 2.01$ in the EPR spectrum (Figure S1). The spectrum of the sample with $^{14}N_2H_4$ (Figure 7A) shows two pairs of cross-features symmetrical relative to the diagonal. Those are extended cross-features **2** of complex shape with several maxima and cross-peaks **1** possessing symmetrical line shape with elliptic contour.

The spectrum of l($^{15}N_2H_4$) (Figure 7B) shows that ^{15}N labeling does not influence the cross-peaks **1**, indicating that they are produced by protein ^{14}N nitrogen. The labeling also leaves a pair of cross-peaks **2″** located in the area where extended cross-features **2** were observed in the spectrum of the sample with $^{14}N_2H_4$. This indicates that the cross-features **2** in Figure 7A result from the contribution of two different types of nitrogens. One contribution, denoted **2′**, is lost in the ^{15}N sample and is from ^{14}N of $^{14}N_2H_4$; the second (**2″**) is from ^{14}N associated with the MoFe protein. In keeping with this assignment, ^{15}N nitrogens of $^{15}N_2H_4$ produce new cross-peaks **3** in Figure 7A, located symmetrically around the diagonal point with ^{15}N Larmor frequency ($^{15}\nu_N$, $^{15}\nu_N$), that correspond to the lost signal **2′**.

The most important aspect of the HYSCORE spectrum Figure 7B is that there is *no* signal around the diagonal point at the ^{15}N Larmor frequency (1.49 MHz) from a very weakly coupled ^{15}N, and the same is true for spectra recorded at other fields. The limit of detectability for a small coupling in HYSCORE is at least as low as that for Mims ENDOR. The absence of *any* trace of a weakly coupled $^{15}N2$ in *either* experiments indicate that the N−N bond of substrate N_2H_4 has been cleaved, and the $^{15}N1$ and $^{1}H1$ ENDOR signals are associated with an [N1H$_y$] species. As discussed below, this conclusion is supported by earlier studies of **I** formed with isotopically labeled NH═N−CH$_3$.[23]

HYSCORE spectra measured for l($^{15}N_2H_4$) at different magnetic fields show that the cross-peaks **1** are present in spectra measured in the field interval from 332.0 mT ($g = 2.087$) up to 364.0 mT ($g = 1.90$) but decay quickly at magnetic fields below $g = 2.01$. This suggestion that the cross-peaks **1** come from nitrogen(s) associated with the 4Fe4S center of the Fe protein was confirmed by HYSCORE examination of the isolated Fe protein. In contrast, the cross-peaks **2″** are observed from the low-field edge of the EPR spectrum ($g = g_1$) up to 352.0 mT ($g = 1.97$) and the cross-peaks **3** from ^{15}N likewise are seen in this field interval, which indicates that the **2″** and **3** (and **2′**) cross-peaks are from nitrogen(s) interacting with FeMo-co of the MoFe intermediate. The width and intensity of these cross-peaks **1** and **2″** are consistent with the cross-correlation of ^{14}N double-quantum transitions from $m_S = \pm 1/2$ manifolds.

Analysis of ^{14}N HYSCORE peaks (1 and 2″). The frequency of double-quantum transition in powder spectra is well described by the following equation:[35]

$$\nu_{dq\pm} = 2[\nu^2_{ef\pm} + \kappa]^{1/2} \quad (3)$$

where $\kappa = K^2(3 + \eta^2)$, $\nu_{ef\pm} = |\nu_N \pm A/2|$. We suggest that $\nu_{dq\pm}$ taken from the spectra obtained in the region of the intermediate g_2-values, where a broad set of orientations contribute to the spectra, would allow an accurate estimate of hyperfine coupling and quadrupole coupling constant $K = e^2Qq/4h$ for nitrogens producing cross-peaks **1** and **2″**. The corresponding frequencies are of (4.0, 3.1) MHz for cross-peaks **1** and (3.81, 2.14) MHz for cross-peaks **2″**. Rearrangement of eq 3 yields the formula:

$$A = ((\nu_{dq+})^2 - (\nu_{dq-})^2)/8\nu_N \quad (4)$$

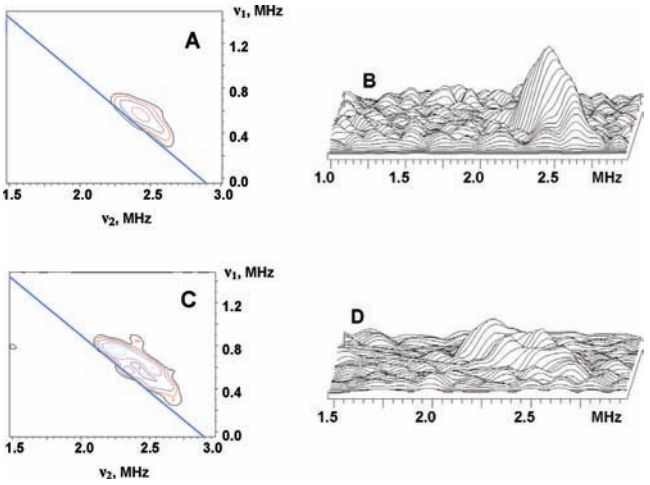

Figure 8. Contour (A,C) and stacked (B, D) presentations of the cross-features **3** from the HYSCORE spectra of the l($^{15}N_2H_4$) intermediate (magnetic field 329.5 mT (A, B) and 332.3 mT (C, D), time between first and second pulses $\tau = 136$ ns, microwave frequency 9.7034 GHz (A, B) and 9.7057 GHz (C, D)).

This equation, together with the corresponding ^{14}N Zeeman frequency, gives couplings $A(^{14}N) = 0.7$ MHz (**1**) and $A(^{14}N) = 1.15$ MHz (**2″**). Using the derived values of the hyperfine coupling, one can calculate the quadrupole parameter from eq 3: $\kappa = K^2(3 + \eta^2) = 1.84$ MHz^2 (**1**) and 0.9 MHz^2 (**2″**). Those correspond to quadrupole coupling constant (qcc) $K = 0.73 \pm 0.05$ MHz (**1**) and $K = 0.5 \pm 0.04$ MHz (**2″**) but do not permit assignment of the asymmetry parameter, $0 \le \eta \le 1$. The qcc (**1**) is consistent with peptide nitrogens H-bonded to the 4Fe4S cluster, which exhibit quadrupole coupling constants, $K \sim 0.7-0.8$ MHz.[36] On the other hand, the lower value of the qcc (**2″**) suggests that FeMo-co center forms a hydrogen bond with another type of nitrogen.

The cross-features **2′** and **2″** significantly overlap in forming feature **2** of the HYSCORE spectra of the l($^{14}N_2H_4$) intermediate, but comparison of Figure 7A and 7B shows that cross-features **2′** possess a more complex extended shape. However, the overlap of the **2′** and **2″** cross-peaks suggests that the values of hyperfine and quadrupole couplings for these two nitrogens are essentially the same, thereby giving for **2′**, $A(^{14}N) \approx 1.15$ MHz, $K \approx 0.5 \pm 0.04$ MHz for the cofactor-bound NH$_y$ fragment. This hyperfine coupling corresponds to $A(^{15}N) \approx 1.6$ MHz, in agreement with $|a_{iso}(^{15}N1)| = 1.8$ MHz derived above from 35 GHz ENDOR spectra. The extended shape of the **2′** cross-peaks correlates with the features in the EPR and ^{15}N ENDOR and ^{15}N HYSCORE (see below) spectra that suggest the presence of several similar conformations of the paramagnetic center.

The estimate of K with an accuracy of ~15% facilitates its assignment to the particular type of nitrogens of the protein environment. Nevertheless, for a complete description of the nuclear−quadrupole interaction tensor, and its unambiguous assignment, direct determination of both quadrupole parameters, K and η, would be desirable. These values could be determined directly from ESEEM experiments satisfying the cancelation condition $\nu_{ef} \sim 0$ at one of the manifolds. For hyperfine coupling $A \sim 0.67-1.0$ MHz, the cancelation condition is reached at ^{14}N Zeeman frequency $\nu_I \sim 0.35-0.5$ MHz, that corresponds to the S-band experiment with microwave frequency ~3−4 GHz.

^{15}N HYSCORE. X-band HYSCORE spectra measured at different magnetic fields across the EPR spectrum of l($^{15}N_2H_4$) all show ^{15}N cross-features (**3**) centered symmetrically around the diagonal point with the ^{15}N Zeeman frequency. Their location corresponds to the ^{15}N hyperfine coupling ~1.5−2.0 MHz (Figure 8), in agreement with the ^{14}N HYSCORE (**2′**) and ^{15}N ENDOR results for the substrate-derived [NH_y]. The shape of the cross-peaks for **3** significantly varies with magnetic field. For instance, the cross-peak **3** in the "single-crystal-like" spectrum recorded near g_1 is a peak with a single maximum and resolved additional shoulders (Figure 8A,B). In contrast, two closely located but resolved ridges are seen in the spectra recorded at the fields between g_1 (low field) and g_2 (maximum intensity) (Figure 8C,D). The complicated shape of these ^{15}N HYSCORE ridges, **3**, corresponds to the extended shape of the ^{14}N features **2′**.

The regression lines of such ridges when plotted as $(\nu_\alpha)^2$ vs $(\nu_\beta)^2$ must form a triangle with the apexes on the $|\nu_\alpha + \nu_\beta| = 2\nu_N$ curve for signals from a single ^{15}N. However, the analysis presented in detail in Supporting Information shows that regression lines for the ridges from Figure 8C,D (and others) do not form such a shape, indicating that the ^{15}N spectra are not consistent with a single nucleus. This is expected, as the ENDOR measurements described above show that metal ion(s) of FeMo-co in the intermediate bind a single nitrogen from substrate, but the intermediate exists in two conformations. The $(\nu_\alpha)^2$ vs $(\nu_\beta)^2$ analysis for the ridges located closer to and farther from to the antidiagonal in Figure 8C,D gives the following estimate for anisotropic components for ^{15}N1 of the two conformers, $T \sim 0.3-0.4$ and $0.6-0.7$ MHz, respectively. The isotropic couplings would be practically the same for both ridges with the value about 1.9−2.1 MHz or − (1.5−1.6) MHz, in satisfactory agreement with $|a_{iso}(^{15}N1)|$ determined by ENDOR. The quantity, $2T$, can be considered as a rough estimate of the maximum component of the anisotropic tensor for these two conformations, giving $T_{max} \sim 0.6-0.8$ MHz and 1.2−1.4 MHz, similar to $T_{max}(N1) = 1.0$ MHz seen in ENDOR.

DISCUSSION

This report describes EPR/ENDOR/HYSCORE measurements of the common intermediate, **I**, formed during freeze-quench of the α-70^{Ala}/α-195^{Gln}-substituted MoFe protein under turnover conditions using N_2H_4, CH_3N_2H, or N_2H_2 as substrate. We first discuss the properties of this intermediate and then incorporate the conclusions we reach into an analysis that leads us to propose that nitrogenase functions by the A reaction pathway of Scheme 1.

Nature of Intermediate I. Earlier X/Q-band EPR and 35 GHz ENDOR measurements showed that freeze-quench of the α-70^{Ala}/α-195^{Gln}-substituted MoFe protein during turnover with N_2H_4 or N_2H_2 causes loss of the EPR signal from resting-state ($S = 3/2$) FeMo-co and the appearance of the signals from low-spin ($S = 1/2$) intermediates with almost axial **g** tensors, originally denoted m(N_2H_2)[17] and l(N_2H_4),[21] respectively. The properties of these intermediates, as measured in the previous work and extended in the present study, establish that they correspond to a common state: [m(N_2H_2), l(N_2H_4)] = **I**. The temperature and microwave power dependencies of the **I** EPR signal indicate that the FeMo-co of this state has two major conformers with different **g** tensors (g_1 = 2.09, 2.11) and significantly different relaxation properties.

^{1,2}H and ^{15}N 35 GHz CW and pulsed ENDOR measurements showed that **I** has an [N_xH_y] fragment bound to FeMo-co.[17] The proton(s) associated this fragment have been investigated here by 35 GHz 2 K CW ^{1,2}H ENDOR and X-band 8 K HYSCORE/ESEEM measurements with samples prepared in H_2O/D_2O buffers. At the microwave power settings used for 2 K Q-band CW ^{1}H ENDOR measurements and at the temperature used for the HYSCORE measurements, each measurement interrogates both conformers of **I** with approximately equal sensitivity. The two techniques confirm that **I** exhibits a signal from exchangeable H1 proton(s) with a maximum hyperfine coupling, $A \sim 9$ MHz, and that the H1 signals can be interpreted in terms of an axial hyperfine tensor with $A_\perp = |a - T| \sim 9$ MHz and $A_{||} = |a + 2T| \sim 4.8$ MHz, corresponding to $T = 4.6$ MHz, $a = -4.3$ MHz (signs are relative).

The 2 K Q-band pulsed ^{15}N ENDOR spectra are collected with short repetition times (~ 10 ms) and are dominated by the g_1 = 2.09 conformer of **I**. A 2D field-frequency pattern of the ^{15}N ENDOR spectra of this **I** conformer can be analyzed in terms of a single bound ^{15}N, with hyperfine tensor, **A**(^{15}N1) = ±[1, 1.5, 2.8] MHz, although the spectra appear to be distorted by contributions from the single ^{15}N1 of the second conformer. The 8 K X-band ^{15}N HYSCORE measurements are consistent with this tensor, but the shape of the HYSCORE signal appears to represent comparable contributions from two nitrogens with very similar couplings. As the 8 K HYSCORE measurement is equally sensitive to signals from the two conformers, these experiments are consistent with the view that the ^{15}N ENDOR and HYSCORE responses do not arise from a [$^{15}N_2H_y$] species with roughly equivalent ^{15}N bound to FeMo-co, and instead each of the two slightly different ^{15}N is associated with one of the conformers of the FeMo-co center. This interpretation is confirmed by experiments with **I** formed from specifically labeled $CH_3-N=^{15}N-H$ and $CH_3-^{15}N=N-H$ as substrates. The ^{15}N ENDOR signals from the single ^{15}N of $CH_3-N=^{15}N-H$ are identical to those of **I** formed from the other two substrates, Figure 5A, and no such signal is seen when $CH_3-^{15}N=N-H$ is employed.[23] These results prove that the two contributing ^{15}N represent a single nitrogen from substrate bound to FeMo-co metal ion(s), but with properties that differ slightly in the two conformers. The ^{14}N HYSCORE patterns for **I** further give the quadrupole coupling parameter for N1, $K \approx 0.5 \pm 0.04$ MHz.

The conclusion that the ^{15}N1 signals originate from a single nitrogen atom bound to a metal ion(s) of FeMo-co leads to the question of whether or not the substrate-derived species retains the N−N bond of the N_2H_4/N_2H_2 substrates. If the second N is present but not bound to a metal ion, it would have a weaker hyperfine coupling. High-resolution 35 GHz pulsed ENDOR spectra (Figure 6) show *no* evidence of a weakly coupled ^{15}N2. We estimate that a second ^{15}N2 could be present only if it had a hyperfine coupling at least 40-fold smaller than that of the observed ^{15}N1 signal; as a comparison, preliminary results indicate that the coupling constant of the remote ^{15}N2 of $^{15}N_2H_4$ bound to the ferriheme of heme oxygenase[37] is roughly 20-fold less than that of the ^{15}N1 bound to Fe. The HYSCORE experiment likely has an even lower threshold than ENDOR for the detection of a weakly bound ^{15}N, and it also shows *no* response from a second nitrogen atom. Finally, when **I** is trapped during turnover with the selectively labeled $CH_3-^{15}N=NH$, $^{13}CH_3-N=NH$, or $C^2H_3-N=NH$, no signal is seen from the isotopic labels.[23] From these results we conclude that the N=N bonds of N_2H_2 and CH_3N_2H, and the N−N bond of N_2H_4, have been broken in forming the common

EPR-active intermediate **I** during enzymatic turnover. This intermediate thus contains an $[NH_y]$ moiety bound to FeMo-co and when useful can be denoted as **I**$[NH_y]$.

The Nitrogenase Reaction Pathway. On the basis of the alternative reaction pathways pictured in Scheme 1, the $[NH_y]$ moiety bound to FeMo-co of **I** could be $[{=}NH]$, $[{-}NH_2]$, or even the product $[NH_3]$ (not shown). Given that two of the states that bind these fragments are reached by both pathways, the *nature* of this moiety does not in itself distinguish between A and D pathways. However, the present findings in conjunction with other considerations lead us to propose that nitrogenase functions via the A reaction pathway of Scheme 1 for reduction of N_2.

Both N_2H_2 and N_2H_4 are substrates that are reduced to two NH_3 by the wild-type nitrogenase. By opening the reactive site, the α-70^{Ala} substitution merely enhances the reduction of these substrates, while the α-195^{Gln} substitution further favors the trapping of **I**$[NH_y]$. The reduction of N_2H_4 must begin by its binding to FeMo-co, and this necessarily generates a state associated only with the A pathway, as there is no N_2H_4-bound intermediate along D. Instead, according to the D pathway, Scheme 1, the N−N bond is cleaved two stages of hydrogenation prior to the appearance of an intermediate at the formal reduction stage of N_2H_4. In contrast, diazenido intermediates exist on both routes. To explain how nitrogenase could reduce each of the substrates, N_2, N_2H_2, and N_2H_4, to two NH_3 molecules via a common A reaction pathway, one need only postulate that each substrate 'joins' the pathway at the appropriate stage of reduction, binding to FeMo-co that has been 'activated' by accumulation of a sufficient number of electrons (possibly with FeMo-co reorganization) and then proceeds along that pathway. For N_2H_2 to instead join the D pathway would imply that it is converted to the $[NH_2{=}N]$ tautomeric form upon binding to FeMo-co, a seemingly implausible process. Moreover, the strong influence of α-70^{Val} substitutions of MoFe protein on substrate access *without* modification of FeMo-co reactivity strongly implicates Fe, rather than Mo, as the site of binding and reactivity,[19] and energetic considerations then implicate the A pathway.[12] Overall, the combination of these considerations with the finding of the formation of the common intermediate **I** thus lead us to conclude that N_2H_2, CH_3N_2H, and N_2H_4 are all reduced by the common A pathway.

Does that require N_2 reduction to follow the same pathway? Rejection of the D pathway contradicts the suggestions of an early study[8] which showed that hydrazine is released upon acid or base quenching of nitrogenase actively reducing dinitrogen.[9] This finding was interpreted as indicating that the diazenido intermediate in the D pathway (Scheme 1) can be viewed as accepting two electrons from FeMo-co, making it a hydrazido dianion $(N{-}NH_2^{2-})$, and that this dianionic species is protonated and released as N_2H_4 upon hydrolysis by *either* acid or base. However, it is clearly more economical[38] to propose that the hydrazine observed during acid/base quenching of nitrogenase is merely released from the hydrazine-bound intermediate that occurs naturally as a stage along the A pathway, Scheme 1, *and* that all nitrogenous substrates, N_2 included, undergo reduction to two NH_3 molecules by the common pathway, A. Likewise, it is most economical to suggest that both the Mo-dependent nitrogenase studied here and the V-dependent nitrogenase[4] reduce N_2 by the same pathway. As it has been shown that V-nitrogenase produces N_2H_4 while reducing N_2,[39] then according to Scheme 1 this enzyme clearly functions via the A pathway, implying the same is true for Mo-nitrogenase.

No nitrogenous substrate binds to resting-state (S = 3/2) FeMo-co of nitrogenase,[40] so the activation of FeMo-co for each substrate requires the accumulation of some requisite number of electrons. The most refractory substrate is N_2 itself, and the Lowe−Thorneley scheme states that the accumulation of three, and most effectively four, electrons is required to bind N_2 and initiate its reduction.[3,9,10] Indeed, our previous work characterized the intermediate that has accumulated four electrons.[19,41] Presumably, lower numbers of accumulated electrons are required to initiate reduction of N_2H_2 and N_2H_4, as is true for reduction of C_2H_2.[3,9]

CONCLUSIONS

(i) EPR/ENDOR/HYSCORE measurements establish that a common intermediate, **I**, is trapped during turnover of N_2H_2, CH_3N_2H, or N_2H_4 as substrate for the α-70^{Ala}/α-195^{Gln}-substituted MoFe protein. These measurements reveal that **I** represents a stage of N_2 fixation in which the N−N bond has been cleaved and in which $[{=}NH]$, $[{-}NH_2]$, or even the product $[NH_3]$ are bound to FeMo-co. (ii) Considerations of these findings lead us to conclude that nitrogenase reduces N_2H_2, CH_3N_2H, and N_2H_4 via the A reaction pathway presented in Scheme 1, and that the same is true for N_2 itself. Energetic considerations,[12] in combination with the strong influence of α-70^{Val} substitutions of MoFe protein *without* modification of FeMo-co reactivity, then implicate Fe, rather than Mo, as the site of binding and reactivity.[19]

ASSOCIATED CONTENT

Supporting Information. Two figures including one of X-band pulsed EPR spectra and one of Q-band ^{1}H ENDOR spectra; discussions of 1D ^{1}H four-pulse ESEEM and of ^{1}H and ^{15}N HYSCORE analysis; three figures. This material is available free of charge via the Internet at http://pubs.acs.org.

AUTHOR INFORMATION

Corresponding Author
bmh@northwestern.edu

Present Addresses
[△]Department of Bioproducts and Biosystems Engineering, University of Minnesota, St. Paul, MN 55108.

ACKNOWLEDGMENT

This work has been supported by the NIH (HL 13531, B.M.H.; GM 59087, D.R.D. and L.C.S.; GM 62954, S.A.D.) and NSF (MCB 0723330, B.M.H.).

REFERENCES

(1) Smil, V. *Enriching the Earth: Fritz Haber, Carl Bosch, and the Transformation of World Food Production*; MIT Press: Cambridge, MA, 2001.

(2) Christiansen, J.; Dean, D. R.; Seefeldt, L. C. *Annu. Rev. Plant Physiol. Plant Mol. Biol.* **2001**, *52*, 269–295.

(3) Burgess, B. K.; Lowe, D. J. *Chem. Rev. (Washington, DC, U. S.)* **1996**, *96*, 2983–3011.

(4) Eady, R. R. *Chem. Rev. (Washington, D. C.)* **1996**, *96*, 3013–3030.

(5) Seefeldt, L. C.; Hoffman, B. M.; Dean, D. R. *Annu. Rev. Biochem.* **2009**, *78*, 701–722.

(6) Hoffman, B. M.; Dean, D. R.; Seefeldt, L. C. *Acc. Chem. Res.* **2009**, *42*, 609–619.

(7) Chatt, J.; Dilworth, J. R.; Richards, R. L. *Chem. Rev.* **1978**, *78*, 589–625.
(8) Thorneley, R. N. F.; Eady, R. R.; Lowe, D. J. *Nature* **1978**, *272*, 557–558.
(9) Thorneley, R. N. F.; Lowe, D. J. In *Molybdenum Enzymes*; Spiro, T. G., Ed.; Wiley-Interscience: New York, 1985; Vol. 7, pp 89−116.
(10) Wilson, P. E.; Nyborg, A. C.; Watt, G. D. *Biophys. Chem.* **2001**, *91*, 281–304.
(11) Schrock, R. R. *Acc. Chem. Res.* **2005**, *38*, 955–962.
(12) Neese, F. *Angew. Chem., Int. Ed.* **2006**, *45*, 196–199.
(13) Kastner, J.; Blochl Peter, E. *J. Am. Chem. Soc.* **2007**, *129*, 2998–3006.
(14) Hinnemann, B.; Norskov, J. K. *Top. Catal.* **2006**, *37*, 55–70.
(15) Burgess, B. K. in *Metal Ions in Biology: Molybdenum Enzymes*; Spiro, T. G., Ed.; John Wiley and Sons: New York, 1985; pp 161−220.
(16) Barney, B. M.; Lukoyanov, D.; Igarashi, R. Y.; Laryukhin, M.; Yang, T.-C.; Dean, D. R.; Hoffman, B. M.; Seefeldt, L. C. *Biochemistry* **2009**, *48*, 9094–9102.
(17) Barney, B. M.; McClead, J.; Lukoyanov, D.; Laryukhin, M.; Yang, T. C.; Hoffman, B. M.; Dean, D. R.; Seefeldt, L. C. *Biochemistry* **2007**, *46*, 6784–6794.
(18) Lee, H.-I.; Igarashi, R. Y.; Laryukhin, M.; Doan, P. E.; Dos Santos, P. C.; Dean, D. R.; Seefeldt, L. C.; Hoffman, B. M. *J. Am. Chem. Soc.* **2004**, *126*, 9563–9569.
(19) Igarashi, R. Y.; Laryukhin, M.; Santos, P. C. D.; Lee, H.-I.; Dean, D. R.; Seefeldt, L. C.; Hoffman, B. M. *J. Am. Chem. Soc.* **2005**, *127*, 6231–6241.
(20) Barney, B. M.; Igarashi, R. Y.; Dos Santos, P. C.; Dean, D. R.; Seefeldt, L. C. *J. Biol. Chem.* **2004**, *279*, 53621–53624.
(21) Barney, B. M.; Laryukhin, M.; Igarashi, R. Y.; Lee, H.-I.; Santos, P. C. D.; Yang, T.-C.; Hoffman, B. M.; Dean, D. R.; Seefeldt, L. C. *Biochemistry* **2005**, *44*, 8030–8037.
(22) Barney, B. M.; Yang, T.-C.; Igarashi, R. Y.; Santos, P. C. D.; Laryukhin, M.; Lee, H.-I.; Hoffman, B. M.; Dean, D. R.; Seefeldt, L. C. *J. Am. Chem. Soc.* **2005**, *127*, 14960–14961.
(23) Barney, B. M.; Lukoyanov, D.; Yang, T.-C.; Dean, D. R.; Hoffman, B. M.; Seefeldt, L. C. *Proc. Natl. Acad. Sci. U.S.A.* **2006**, *103*, 17113–17118.
(24) Barney, B. M.; Lee, H.-I.; Dos Santos, P. C.; Hoffman, B. M.; Dean, D. R.; Seefeldt, L. C. *Dalton Trans.* **2006**, 2277–2284.
(25) Kim, C.-H.; Newton, W. E.; Dean, D. R. *Biochemistry* **1995**, *34*, 2798–2808.
(26) Lowe, D. J. *ENDOR and EPR of Metalloproteins*; R. G. Landes Co.: Austin, TX, 1995.
(27) Hoffman, B. M. *Acc. Chem. Res.* **2003**, *36*, 522–529.
(28) Schweiger, A.; Jeschke, G. *Principles of Pulse Electron Paramagnetic Resonance*; Oxford University Press: Oxford, UK, 2001.
(29) DeRose, V. J.; Hoffman, B. M. In *Methods Enzymol.*; Sauer, K., Ed.; Academic Press: New York, 1995; Vol. 246, pp 554−589.
(30) Doan, P. E.; Hoffman, B. M. *Chem. Phys. Lett.* **1997**, *269*, 208–214.
(31) Hoefer, P.; Grupp, A.; Nebenfuehr, H.; Mehring, M. *Chem. Phys. Lett.* **1986**, *132*, 279–282.
(32) Dikanov, S. A.; Bowman, M. K. *J. Magn. Res. Ser. A* **1995**, *116*, 125–128.
(33) Dikanov, S. A.; Bowman, M. K. *JBIC, J. Biol. Inorg. Chem.* **1998**, *3*, 18–29.
(34) Jin, H.; Turner, I. M., Jr.; Nelson, M. J.; Gurbiel, R. J.; Doan, P. E.; Hoffman, B. M. *J. Am. Chem. Soc.* **1993**, *115*, 5290–5291.
(35) Dikanov, S. A.; Tsvetkov, Y. D.; Bowman, M. K.; Astashkin, A. V. *Chem. Phys. Lett.* **1982**, *90*, 149–153.
(36) Dikanov, S. A.; Samoilova, R. I.; Kappl, R.; Crofts, A. R.; Hüttermann, J. *Phys. Chem. Chem. Phys.* **2009**, *11*, 6807–6819.
(37) Sakamoto, H.; Higashimoto, Y.; Hayashi, S.; Sugishima, M.; Fukuyama, K.; Palmer, G.; Noguchi, M. *J. Inorg. Biochem.* **2004**, *98*, 1223–1228.
(38) "Occam's razor", *Wikipedia-Contributors Wikipedia, The Free Encyclopedia*, http://en.wikipedia.org/w/index.php?title=Occam%27s_razor&oldid=418788633 (accessed March 16, 2011).
(39) Dilworth, M. J.; Eady, R. R. *Biochem. J.* **1991**, *277*, 465–468.
(40) Benton, P. M. C.; Mayer, S. M.; Shao, J.; Hoffman, B. M.; Dean, D. R.; Seefeldt, L. C. *Biochemistry* **2001**, *40*, 13816–13825.
(41) Lukoyanov, D.; Barney, B. M.; Dean, D. R.; Seefeldt, L. C.; Hoffman, B. M. *Proc. Natl. Acad. Sci. U.S.A.* **2007**, *104*, 1451–1455.